

Article

Novel Quinazolinone–Isoxazoline Hybrids: Synthesis, Spectroscopic Characterization, and DFT Mechanistic Study

Yassine Rhazi ¹, Mohammed Chalkha ¹, Asmae Nakkabi ¹, Imad Hammoudan ², Mohamed Akhazzane ³, Mohamed Bakhouch ⁴, Samir Chtita ^{5,*} and Mohamed El Yazidi ^{1,*}

- ¹ Engineering Laboratory of Organometallic and Molecular Materials and Environment, Faculty of Sciences Dhar EL Mahraz, Sidi Mohamed Ben Abdellah University, Fez P.O. Box 1796, Morocco
- ² Laboratory Physical Chemistry, Faculty of Sciences of Tetouan, Abdelmalk Essaadi University, Tetouan P.O. Box 93002, Morocco
- ³ Cité de l’Innovation, Université Sidi Mohamed Ben Abdellah, Route Immouzer, Fez P.O. Box 2626, Morocco
- ⁴ Laboratory of Bioorganic Chemistry, Department of Chemistry, Faculty of Sciences, Chouaib Doukkali University, El Jadida P.O. Box 24, Morocco
- ⁵ Laboratory of Analytical and Molecular Chemistry, Faculty of Sciences Ben M’Sik, Hassan II University of Casablanca, Casablanca P.O. Box 7955, Morocco
- * Correspondence: samirchtita@gmail.com (S.C.); elyazidimohamed@hotmail.com (M.E.Y.); Tel.: +212-660005554 (S.C.); +212-661488871 (M.E.Y.)

Abstract: Quinazolinone and isoxazoline systems have attracted much attention due to their interesting pharmacological properties. The association of these two pharmacophores in a single hybrid structure can boost the biological activity or bring a new one. Inspired by this new paradigm, in the present work we report the synthesis and spectroscopic characterization of new quinazolinone–isoxazoline hybrids. The target compounds were obtained via 1,3-dipolar cycloaddition reactions of aryl nitriloxides and N-allylquinazolinone. The synthesized compounds were characterized using spectroscopic techniques such as IR, 1D NMR (1H and 13C), 2D NMR (COSY and HSQC), and high-resolution mass spectrometry (HRMS). The spectral data show that this reaction leads only to the 3,5-disubstituted isoxazoline regioisomer, and that the observed regiochemistry is not affected by the nature of the substituents in the phenyl ring of the dipole. In addition, a theoretical study was performed using density functional theory (DFT) to support the experimental results in regard to the regiochemistry of the studied reactions. The computational mechanistic study was in good agreement with the experimental data.

Keywords: N-allylquinazolinone; quinazolinone–isoxazoline hybrids; 1,3-dipolar cycloaddition; theoretical study; regiochemistry



Citation: Rhazi, Y.; Chalkha, M.; Nakkabi, A.; Hammoudan, I.; Akhazzane, M.; Bakhouch, M.; Chtita, S.; El Yazidi, M. Novel Quinazolinone–Isoxazoline Hybrids: Synthesis, Spectroscopic Characterization, and DFT Mechanistic Study. *Chemistry* **2022**, *4*, 969–982. <https://doi.org/10.3390/chemistry4030066>

Received: 3 August 2022

Accepted: 28 August 2022

Published: 30 August 2022

Publisher’s Note: MDPI stays neutral with regard to jurisdictional claims in published maps and institutional affiliations.



Copyright: © 2022 by the authors. Licensee MDPI, Basel, Switzerland. This article is an open access article distributed under the terms and conditions of the Creative Commons Attribution (CC BY) license (<https://creativecommons.org/licenses/by/4.0/>).

1. Introduction

Heterocyclic compounds continue to attract much attention due to their astonishing bioactivity [1–4]. Over the last century, heterocyclic compounds have been widely studied as preferred structures in the investigation of new drug candidates capable of remedying various diseases [5–7]. Oxygen- and nitrogen-containing heterocyclic compounds have gained considerable importance due to their applications in various fields [1,8–10]. Quinazolin-4(3H)-one derivatives, in particular, have occupied a primordial place in medicinal chemistry owing to their wide range of biological activity; namely as antifungal [11,12], antibacterial [11,13], antioxidant [14], antitubercular [11], anticonvulsant [15], and anti-malarial [16] agents, and as potential inhibitors of MERS-CoV and SARS-CoV-2 [2]. Furthermore, they possess insecticidal [17] and fungicidal activities [18]. Due to the excellent biological properties of quinazolin-4(3H)-ones [19,20], as well as their presence in the molecular skeleton of several natural bioactive alkaloids [5,19,21] (Figure 1), many methods devoted to their synthesis have been reported [12,22,23].

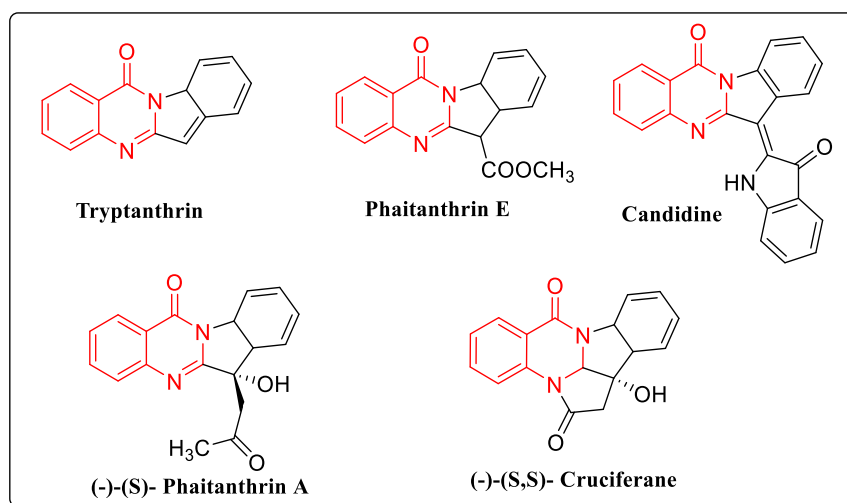


Figure 1. Natural alkaloids containing quinazolinone scaffold.

Moreover, the isoxazoline nucleus has received great attention from researchers owing to its significant pharmacological properties [24]. Indeed, an isoxazoline motif is found in the molecular skeleton of several synthetic and natural compounds used in various fields, including agriculture and medicine [24–27] (Figure 2). Thus, the presence of an isoxazoline ring constitutes a source of motivation in the investigation and design of new therapeutic agent candidates [28,29]. In addition to their interesting properties, such molecules have been used as key intermediates to synthesis a large array of polyfunctional molecules with pharmaceutical interest [28,29]. The synthesis of these heterocyclic compounds is often achieved by cyclocondensation or 1,3-dipolar cycloaddition reactions [30].

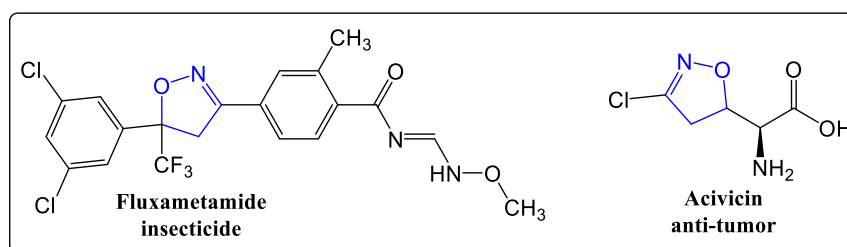


Figure 2. Selected examples of known drugs encompassing an isoxazoline ring.

Recently, molecular hybridization has emerged as a promising approach in designing and developing novel heterocyclic compounds with interesting biological properties [1,8]. The synthesis of new heterocycles based on the hybridization of quinazolinone and isoxazoline pharmacophores is a promising avenue in modern medicinal chemistry [31]. In this regard, and in continuation of our ongoing research focused on the design of new bioactive compounds [32–36], in this work we report the synthesis and characterization of new quinazolinone–isoxazoline hybrids. The synthesis of target compounds **4a–h** was performed using 1,3-dipolar cycloaddition reactions between aryltriloxides **3a–h** and N-allylquinazolinone **2**. We also describe mechanistic and regiochemistry studies of this reaction using density functional theory (DFT) at the B3LYP functional level, with the cc-pVDZ basis set as computational methods.

2. Materials and Methods

2.1. Chemical Reagents and Instruments

All chemicals used were of analytical grade and were purchased from commercial suppliers. The progress of the reactions was monitored by TLC (Merck, silica gel 60 F254), and spots were visualized under UV light (VILBER LOURMAT, VL-215.LC).

Column chromatography was performed using Merck silica gel (70–230 mesh) with n-hexane/ethyl acetate mixtures as eluents. The melting points were determined with an uncertainty of ± 2 °C using a KOFER BENCH. The IR spectra were recorded in the range of 450–4000 cm^{-1} using a BRUKER VERTEX 70 FT-IR spectrometer, and wavenumbers are given in cm^{-1} . The NMR spectra (^1H and ^{13}C) were recorded at room temperature using a BRUKER AVANCE II 300 Ultra-Shield (300 MHz for ^1H and 75 MHz for ^{13}C) spectrometer, employing CDCl_3 as the solvent. The chemical shifts are expressed in ppm, and the coupling constants, J , in Hertz (Hz). The spin multiplicities are reported as singlet (s), doublet (d), triplet (t), multiplet (m), doublet of doublets (dd), doublet of triplets (dt), or broad (br). High-resolution mass spectra were recorded using a Waters/Vion IMS-QTOF spectrometer, equipped with an electrospray ionization (ESI) source operating in either positive or negative ion mode.

Quinazolin-4(3H)-one **1** was prepared according to the literature procedure (white solid, yield 92%, m.p. 214–216 °C (lit., m.p. 214–215 °C)) [37]. 3-allylquinazolin-4(3H)-one **2** was obtained from the condensation reaction of quinazolin-4(3H)-one **1** with allyl bromide in DMF in the presence of sodium hydride, according to the method in previously reported work (white crystals, yield 75%; m.p. 64–66 °C; (lit., m.p. 63–65 °C)) [37]. The NMR spectra of quinazolin-4(3H)-one **1** and 3-allylquinazolin-4(3H)-one **2** are given in the supplementary materials. The arylhydroxamoyl chlorides **3a–h**, as aryl nitriloxide precursors, were prepared following the method described in the literature [38].

2.2. Procedure for the Synthesis of Compounds (4a–h)

In a 100 ml flask, 1 mmol of dipolarophile **2** and 1.2 mmol of arylhydroxamoyl chlorides **3a–h** were dissolved in 40 ml of chloroform. Then, 1.2 mmol of anhydrous triethylamine was added dropwise. Once the addition was complete, the reaction mixture was kept at room temperature under magnetic stirring for the appropriate period of time. Once the reaction was complete, as indicated by TLC, the reaction mixture was transferred into a separatory funnel and washed three times with water. The organic layer was dried over anhydrous sodium sulfate (Na_2SO_4) and filtered, and then the solvent was removed by rotary evaporation. The obtained residue was purified on a silica gel column using a mixture of hexane and ethyl acetate (4:1) as eluent.

3-((3-(4-bromophenyl)-4,5-dihydroisoxazol-5-yl)methyl)quinazolin-4(3H)-one (**4a**):

Yield (96%); m.p.: 194 °C; FT-IR (ν_{max} , cm^{-1}): 3057 ($\text{C}_{\text{Ar}}\text{-H}$), 2923 (C–H), 1670 (C=O), 1610 (C=N), 1562, 1490, 1471 (C=C), 1159 (C–O); ^1H NMR (300 MHz, CDCl_3) (δ /ppm): 8.29 (d, 1H, $J = 7.8$ Hz, Ar–H), 8.17 (s, 1H, N=CH–N), 7.80–7.72 (m, 2H, Ar–H), 7.54–7.48 (m, 5H, Ar–H), 5.20–5.11 (m, 1H, $\text{CH}_{\text{isoxazoline}}$), 4.44 (dd, 1H, $J = 14.1$, 3 Hz, N– CH_2), 4.05 (dd, 1H, $J = 14.1$, 7.5 Hz, N– CH_2), 3.52 (dd, 1H, $J = 17.1$, 10.8 Hz, $\text{CH}_{2\text{isoxazoline}}$), 3.20 (dd, 1H, $J = 17.1$, 6.9 Hz, $\text{CH}_{2\text{isoxazoline}}$). ^{13}C NMR (75 MHz, CDCl_3) (δ /ppm): 161.48 (C=O_{amide}), 156.19 (C=N_{isoxazoline}), 148.14, 146.90 (N=CH–N), 134.56, 132.04, 128.20, 127.73, 127.70, 127.38, 126.63, 124.84, 121.78, 78.63 ($\text{CH}_{\text{isoxazoline}}$), 49.16 (N– CH_2), 37.88 ($\text{CH}_{2\text{isoxazoline}}$); ESI-QTOF-MS (m/z): mass calculated for $[\text{C}_{18}\text{H}_{14}\text{N}_3\text{O}_2\text{Br}+\text{H}]^+$ 384.03331, mass found 384.03367.

3-((3-(4-chlorophenyl)-4,5-dihydroisoxazol-5-yl)methyl)quinazolin-4(3H)-one (**4b**):

Yield (82%); m.p.: 176 °C; FT-IR (ν_{max} , cm^{-1}): 3058 ($\text{C}_{\text{Ar}}\text{-H}$), 2925 (C–H), 1672 (C=O), 1598 (C=N), 1566, 1494, 1471 (C=C), 1159 (C–O); ^1H NMR (300 MHz, CDCl_3) (δ /ppm): 8.31 (d, 1H, $J = 8$ Hz, Ar–H), 8.18 (s, 1H, N=CH–N), 7.80–7.74 (m, 2H, Ar–H), 7.65–7.50 (m, 3H, Ar–H), 7.40–7.37 (d, 2H, $J = 7$ Hz, Ar–H), 5.22–5.12 (m, 1H, $\text{CH}_{\text{isoxazoline}}$), 4.46 (dd, 1H, $J = 14.1$, 3 Hz, N– CH_2), 4.07 (dd, 1H, $J = 14.1$, 7.5 Hz, N– CH_2), 3.54 (dd, 1H, $J = 17.1$, 10.5 Hz, $\text{CH}_{2\text{isoxazoline}}$), 3.22 (dd, 1H, $J = 17.1$, 7.2 Hz, $\text{CH}_{2\text{isoxazoline}}$). ^{13}C NMR (75 MHz, CDCl_3) (δ /ppm): 161.47 (C=O_{amide}), 156.11 (C=N_{isoxazoline}), 148.03, 146.92 (N=CH–N), 136.55, 134.61, 129.11, 128.02, 127.65, 127.44, 127.28, 126.66, 121.76, 78.59 ($\text{CH}_{\text{isoxazoline}}$), 49.19 (N– CH_2), 37.96 ($\text{CH}_{2\text{isoxazoline}}$); ESI-QTOF-MS (m/z): mass calculated for $[\text{C}_{18}\text{H}_{14}\text{N}_3\text{O}_2\text{Cl}+\text{H}]^+$ 340.08404, mass found 340.08417.

3-((3-(4-methoxyphenyl)-4,5-dihydroisoxazol-5-yl)methyl)quinazoline-4(3H)-one (**4c**):

Yield (74%); m.p.: 210 °C; FT-IR (ν_{\max} , cm^{-1}): 3080 ($\text{C}_{\text{Ar}}\text{-H}$), 2954 (C-H), 1666 (C=O), 1600 (C=N), 1562, 1504, 1469 (C=C), 1159 (C-O); ^1H NMR (300 MHz, CDCl_3) (δ/ppm): 8.32 (d, 1H, $J = 8.1$ Hz, Ar-H), 8.19 (s, 1H, N=CH-N), 7.82–7.74 (m, 2H, Ar-H), 7.67 (d, 2H, $J = 2.1$ Hz, Ar-H), 7.56–7.50 (m, 2H, Ar-H), 6.94 (d, 1H, $J = 8.7$ Hz, Ar-H), 5.19–5.10 (m, 1H, $\text{CH}_{\text{isoxazoline}}$), 4.45 (dd, 1H, $J = 14.1, 3$ Hz, N-CH_2), 4.05 (dd, 1H, $J = 14.1, 7.5$ Hz, N-CH_2), 3.95 (s, 3H, $-\text{OCH}_3$), 3.52 (dd, 1H, $J = 16.8, 10.5$ Hz, $\text{CH}_{2\text{isoxazoline}}$), 3.19 (dd, 1H, $J = 16.8, 6.9$ Hz, $\text{CH}_{2\text{isoxazoline}}$); ^{13}C NMR (75 MHz, CDCl_3) (δ/ppm): 161.49 ($\text{C=O}_{\text{amide}}$), 156.63 ($\text{C=N}_{\text{isoxazoline}}$), 155.67 ($>\text{C-OCH}_3$), 148.12, 146.94 (N=CH-N), 134.56, 128.67, 127.69, 127.39, 126.66, 123.05, 122.17, 111.90, 78.35 ($\text{CH}_{\text{isoxazoline}}$), 56.28 ($-\text{OCH}_3$), 49.18 (N-CH_2), 38.09 ($\text{CH}_{2\text{isoxazoline}}$); ESI-QTOF-MS (m/z): mass calculated for $[\text{C}_{19}\text{H}_{17}\text{N}_3\text{O}_3+\text{H}]^+$ 336.12871, mass found 336.13332.

3-((3-(4-nitrophenyl)-4,5-dihydroisoxazol-5-yl)methyl)quinazoline-4(3H)-one (**4d**):

Yield (84%); m.p.: 236 °C; FT-IR (ν_{\max} , cm^{-1}): 3047 ($\text{C}_{\text{Ar}}\text{-H}$), 2941 (C-H), 1662 (C=O), 1610 (C=N), 1579, 1514, 1473 (C=C), 1159 (C-O); ^1H NMR (300 MHz, CDCl_3) (δ/ppm): 8.30–8.24 (m, 3H, Ar-H), 8.18 (s, 1H, N=CH-N), 7.84–7.74 (m, 4H, Ar-H), 7.56–7.51 (m, 1H, Ar-H), 5.32–5.21 (m, 1H, $\text{CH}_{\text{isoxazoline}}$), 4.47 (dd, 1H, $J = 14.1, 3.3$ Hz, N-CH_2), 4.17 (dd, 1H, $J = 14.1, 10.5$ Hz, N-CH_2), 3.59 (dd, 1H, $J = 17.1, 7.2$ Hz, $\text{CH}_{2\text{isoxazoline}}$), 3.31 (dd, 1H, $J = 17.1, 7.2$ Hz, $\text{CH}_{2\text{isoxazoline}}$); ^{13}C NMR (75 MHz, CDCl_3) (δ/ppm): 161.51 ($\text{C=O}_{\text{amide}}$), 155.54 ($\text{C=N}_{\text{isoxazoline}}$), 148.71 (C-NO_2), 147.89, 146.77 (N=CH-N), 134.79, 134.72, 127.68, 127.55, 126.67, 124.06, 121.71, 79.50 ($\text{CH}_{\text{isoxazoline}}$), 49.05 (N-CH_2), 37.53 ($\text{CH}_{2\text{isoxazoline}}$); ESI-QTOF-MS (m/z): mass calculated for $[\text{C}_{18}\text{H}_{14}\text{N}_4\text{O}_4+\text{H}]^+$ 351.10846, mass found 351.10835

3-((3-(p-tolyl)-4,5-dihydroisoxazol-5-yl)methyl)quinazoline-4(3H)-one (**4e**):

Yield (92%); m.p.: 174 °C; FT-IR (ν_{\max} , cm^{-1}): 3033 ($\text{C}_{\text{Ar}}\text{-H}$), 2949 (C-H), 1674 (C=O), 1612 (C=N), 1564, 1515, 1473 (C=C), 1159 (C-O); ^1H NMR (300 MHz, CDCl_3) (δ/ppm): 8.34–8.30 (m, 1H, Ar-H), 8.20 (s, 1H, N=CH-N), 7.79–7.74 (m, 2H, Ar-H), 7.57–7.50 (m, 3H, Ar-H), 7.28–7.20 (m, 2H, Ar-H), 5.16–5.09 (m, 1H, $\text{CH}_{\text{isoxazoline}}$), 4.47 (dd, 1H, $J = 14.1, 3.3$ Hz, N-CH_2), 4.01 (dd, 1H, $J = 14.1, 7.8$ Hz, N-CH_2), 3.56 (dd, 1H, $J = 17.1, 10.5$ Hz, $\text{CH}_{2\text{isoxazoline}}$), 3.20 (dd, 1H, $J = 17.1, 6.9$ Hz, $\text{CH}_{2\text{isoxazoline}}$), 2.39 (s, 3H, CH_3); ^{13}C NMR (75 MHz, CDCl_3) (δ/ppm): 161.46 ($\text{C=O}_{\text{amide}}$), 156.94 ($\text{C=N}_{\text{isoxazoline}}$), 148.11, 147.01 (N=CH-N), 140.87, 134.52, 129.52, 127.66, 127.34, 126.75, 126.66, 125.95, 121.97, 78.07 ($\text{CH}_{\text{isoxazoline}}$), 49.30 (N-CH_2), 38.25 ($\text{CH}_{2\text{isoxazoline}}$); 21.48 (CH_3); ESI-QTOF-MS (m/z): mass calculated for $[\text{C}_{19}\text{H}_{17}\text{N}_3\text{O}_2+\text{H}]^+$ 320.13908, mass found 320.13944.

3-((3-phenyl)-4,5-dihydroisoxazol-5-yl)methyl)quinazoline-4(3H)-one (**4f**):

Yield (59%); m.p.: 166 °C; FT-IR (ν_{\max} , cm^{-1}): 3055 ($\text{C}_{\text{Ar}}\text{-H}$), 2956 (C-H), 1662 (C=O), 1608 (C=N), 1564, 1498, 1469 (C=C), 1190 (C-O); ^1H NMR (300 MHz, CDCl_3) (δ/ppm): 8.34–8.30 (d, 1H, Ar-H), 8.19 (s, 1H, N=CH-N), 7.82–7.73 (m, 2H, Ar-H), 7.68–7.65 (m, 2H, Ar-H), 7.55–7.50 (m, 1H, Ar-H), 7.46–7.44 (m, 3H, Ar-H), 5.20–5.11 (m, 1H, $\text{CH}_{4\text{sooxazoline}}$), 4.48 (dd, 1H, $J = 14.1, 3.0$ Hz, N-CH_2), 4.04 (dd, 1H, $J = 14.1, 7.5$ Hz, N-CH_2), 3.58 (dd, 1H, $J = 16.8, 10.5$ Hz, $\text{CH}_{2\text{isoxazoline}}$), 3.23 (dd, 1H, $J = 16.8, 6.9$ Hz, $\text{CH}_{2\text{isoxazoline}}$); ^{13}C NMR (75 MHz, CDCl_3) (δ/ppm): 161.51 ($\text{C=O}_{\text{amide}}$), 156.99 ($\text{C=N}_{\text{isoxazoline}}$), 148.14, 146.98 (N=CH-N), 134.54, 130.54, 128.82, 127.68, 127.36, 126.81, 126.66, 121.81, 78.28 ($\text{CH}_{4\text{sooxazoline}}$), 49.26 (N-CH_2), 38.13 ($\text{CH}_{2\text{isoxazoline}}$); ESI-QTOF-MS (m/z): mass calculated for $[\text{C}_{18}\text{H}_{15}\text{N}_3\text{O}_2+\text{H}]^+$ 306.12337, mass found 306.12318.

3-((3-(2-chlorophenyl)-4,5-dihydroisoxazol-5-yl)methyl)quinazoline-4(3H)-one (**4g**):

Yield (91%); m.p.: 168 °C; FT-IR (ν_{\max} , cm^{-1}): 3072 ($\text{C}_{\text{Ar}}\text{-H}$), 2962 (C-H), 1670 (C=O), 1608 (C=N), 1562, 1471, 1433 (C=C), 1157 (C-O); ^1H NMR (300 MHz, CDCl_3) (δ/ppm): 8.33 (dd, 1H, $J = 8.1, 1.2$ Hz, Ar-H), 8.21 (s, 1H, N=CH-N), 7.83–7.75 (m, 2H, Ar-H), 7.56–7.51 (m, 2H, Ar-H), 7.42–7.28 (m, 3H, Ar-H), 5.24–5.15 (m, 1H, $\text{CH}_{\text{isoxazoline}}$), 4.43 (dd, 1H, $J = 14.1, 3$ Hz, N-CH_2), 4.12 (dd, 1H, $J = 14.1, 7.5$ Hz, N-CH_2), 3.68 (dd, 1H, $J = 17.1, 10.5$ Hz, $\text{CH}_{2\text{isoxazoline}}$), 3.44 (dd, 1H, $J = 17.1, 6.3$ Hz, $\text{CH}_{2\text{isoxazoline}}$); ^{13}C NMR (75 MHz, CDCl_3)

(δ /ppm): 161.46 (C=O_{amide}), 157.01 (C=N_{isoxazoline}), 148.11, 146.98 (N=CH-N), 134.54, 132.87, 130.54, 128.35, 127.66, 127.38, 127.07, 126.66, 121.87, 78.83 (CH_{isoxazoline}), 49.09 (N-CH₂), 40.51 (CH_{2isoxazoline}); ESI-QTOF-MS (m/z): mass calculated for [C₁₈H₁₄N₃O₂Cl+H]⁺ 340.08430, mass found 340.08428.

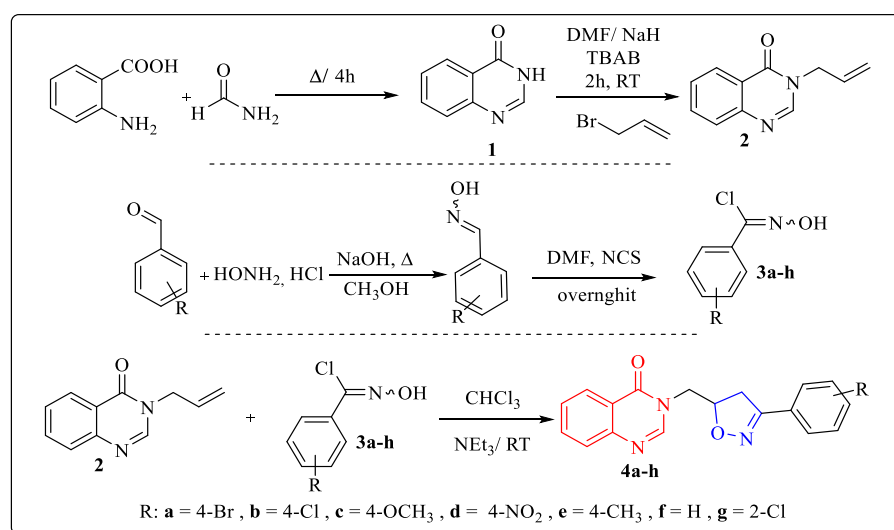
2.3. Computational Details

Currently, density functional theory (DFT) is considered to be the most widely used method, as it gives realistic and reliable results in reproducing experimental regio- and stereoselectivity cycloaddition reactions [39–43]. Therefore, the geometry optimizations of the stationary points were carried out using DFT methods at the B3LYP/cc-pVDZ level theory [44]. The use of the cc-pVDZ base has been shown to give good results in many works [43,45]. We confirmed the active sites through the electrophilic function indices of Parr (Pr⁺) [46,47]. The transition state theory (TST) developed in 1935 by Eyring is the most widely used theory for calculating reaction rates [48,49]; thus, qstn was used to locate the structure of the transition state [50]. The IRC was calculated to give the reaction path according to the coordinates of the reaction [51]. The QTAIM method was used to highlight the topology of the molecular structures [52]. All calculations were carried out with Gaussian 09 software [53].

3. Results and Discussion

3.1. Synthesis and Characterization

The presence of heterocyclic compounds in the main structural motif of a variety of biologically active, natural, and synthetic molecules has encouraged researchers to develop new methods for their synthesis. In this context, we have been interested in the synthesis of aza-heterocyclic derivatives with potential biological activities, using easy and reproducible synthesis strategies [32–35]. In the present work, we describe the synthesis of quinazolin-4(3H)-one-isoxazoline hybrids according to the pathway shown in Scheme 1. Quinazolin-4(3H)-one **1** was obtained by the condensation of anthranilic acid onto formamide, according to a published procedure [37]. It was then reacted with allyl bromide in *N,N*-dimethylformamide (DMF) in the presence of sodium hydride (NaH) and tetra-*N*-butylammonium bromide (TBAB) to result in the formation of *N*-allylated quinazolin-4(3H)-one **2** [37]. TBAB (Bu₄NBr) was used as a phase transfer catalyst to enhance the yield of the reaction. The intermediate **2** was subjected to a series of aryl-nitriloxides to synthesize the targeted compounds **4a–h**. The aryl-nitriloxides were generated in situ from hydroxamoyl chlorides **3a–h** in chloroform at room temperature in the presence of triethylamine [54].



Scheme 1. Synthetic strategy for the preparation of quinazolinone–isoxazoline hybrids **4a–h**.

The structures and regiochemistries of the synthesized compounds were established from spectroscopic data. The physical properties and spectroscopic data of all synthesized products are summarized in Table 1. The analysis of NMR data in all studied cases reveals that the reaction led to the formation of one regio-isomer only, regardless of the donor or attractor nature of the substituent carried by the phenyl ring of the dipole.

Table 1. Physical properties and spectroscopic data of compounds **4a–g**.

Entry	R	Formula (M. g/mol)	M.p. (°C)	Yield ^a (%)	NMR-1H (ppm)	13C-NMR (ppm)	IR (cm ⁻¹)	HRMS(<i>m/z</i>) [M+H] ⁺
					N-CH ₂ CH ₂ (isoxazoline) CH(isoxazoline)	N-CH ₂ CH ₂ CH	C=O C=N	
4a	4-Br	C ₁₈ H ₁₄ N ₃ O ₂ Br (383.03)	194	96	4.05 (dd, 1H); 4.44 (dd, 1H) 3.20 (dd, 1H); 3.52 (dd, 1H) 5.11–5.20 (m, 1H)	49.16 37.88 78.63	1670 1610	384.03367
4b	4-Cl	C ₁₈ H ₁₄ N ₃ O ₂ Cl (339.08)	176	82	4.08 (dd, 1H); 4.46 (dd, 1H) 3.23 (dd, 1H); 3.54 (dd, 1H) 5.12–5.22 (m, 1H)	49.15 37.95 78.63	1672 1598	340.08417
4c	4-OCH ₃	C ₁₉ H ₁₇ N ₃ O ₃ (335.13)	210	74	4.05 (dd, 1H); 4.46 (dd, 1H) 3.19 (dd, 1H); 3.53 (dd, 1H) 5.10–5.19 (m, 1H)	49.19 37.96 78.59	1666 1600	336.13332
4d	4-NO ₂	C ₁₈ H ₁₄ N ₄ O ₄ (350.1)	236	84	4.17 (dd, 1H); 4.47 (dd, 1H) 3.31 (dd, 1H); 3.59 (dd, 1H) 5.21–5.32 (m, 1H)	49.16 37.88 78.63	1662 1610	351.10835
4e	4-CH ₃	C ₁₉ H ₁₇ N ₃ O ₂ (319.13)	174	92	4.01 (dd, 1H); 4.47 (dd, 1H) 3.21 (dd, 1H); 3.56 (dd, 1H) 5.09–5.18 (m, 1H)	49.30 38.25 78.07	1674 1612	320.13944
4f	H	C ₁₈ H ₁₅ N ₃ O ₂ (305.12)	166	59	4.45 (dd, 1H); 4.04 (dd, 1H) 3.34 (dd, 1H); 3.58 (dd, 1H) 5.11–5.20 (m, 1H)	49.26 38.13 78.28	1662 1608	306.12318
4g	2-Cl	C ₁₈ H ₁₄ N ₃ O ₂ Cl (339.08)	168	91	4.12 (dd, 1H); 4.43 (dd, 1H) 3.44 (dd, 1H); 3.68 (dd, 1H) 5.15–5.24 (m, 1H)	49.09 40.51 78.83	1670 1608	340.08428

^a Yield of products after purification.

The mass spectra of the newly synthesized hybrid molecules showed the existence of a molecular ion peak [M+H]⁺ corresponding to the exact mass of the single molecule consistent with the chemical formula of the proposed structures. For example, the mass spectrum of compound **4a** shows a peak for the protonated molecular ion [M+H]⁺ at *m/z*: 384.03331, which affirms the molecular formula [C₁₈H₁₄N₃O₂Br] of the proposed structure (Figure S10). In addition, the FT-IR spectrum of compound **4a** reveals the presence of two absorption bands that appear at approximately 1159 cm⁻¹ and 1610 cm⁻¹, characteristic of the vibrations of the C–O and C=N bonds of the isoxazoline nucleus, respectively. It also shows the existence of another absorption band at 1670 cm⁻¹, attributed to the vibration of the C=O bond of the carbonyl of the quinazolin-4(3H)-one ring.

In the ¹H-NMR spectrum of compound **4a** (Figure S5), we note the presence of four signals as a doublet of doublets (dd), attributable to the four diastereotopic hydrogens attached to the two methylene groups neighboring the stereogenic center. The doublet of doublets centered at 4.05 ppm and 4.44 ppm corresponds to the two protons of the methylene group near the nitrogen atom (N–CH₂), whereas the two other doublets of doublets at 3.20 ppm and 3.52 ppm are attributed to the two hydrogen atoms of the methylene group belonging to isoxazoline ring. The presence of a multiplet signal in the spectrum of compound **4a** between 5.11 and 5.20 ppm is consistent with the chemical shift of the H₅ proton of the 3,5-disubstituted isoxazoline regioisomer (Figure 3). The chemical shift value of the H₅ proton of the isoxazoline ring is in good agreement with that found for similar structures in the literature [28,55,56]. The singlet signal at 8.17 ppm is

attributed to the proton of methine group (=CH-) attached to the two nitrogen atoms of quinazolin-4(3H)-one.

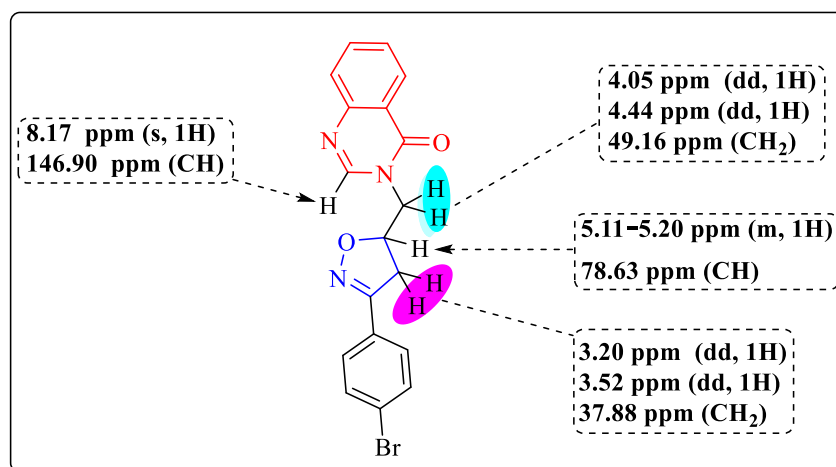


Figure 3. Characteristic signals in the ^1H and ^{13}C NMR spectra of compound **4a**.

The ^{13}C -NMR spectrum of compound **4a** (Figure S7) shows the presence of three signals located at 37.88 ppm, 78.63 ppm, and 156.19 ppm, attributed to carbons of the methylene (CH_2), methine (CH), and imine ($\text{C}=\text{N}$) groups of the isoxazoline nucleus, respectively. These chemical shift values are in good agreement with the literature, and confirm the formation of 3,5-disubstituted isoxazoline as a single regioisomer [28,55,56]. Other signals located at 146.90 ppm and 161.48 ppm are assigned to the methine ($\text{N}=\text{CH}-\text{N}$) and carbonyl ($\text{C}=\text{O}$) carbons of quinazolin-4(3H)-one, respectively. The signal at 49.16 ppm corresponds to the methylene carbon (CH_2) that links the isoxazoline ring with the quinazolin-4(3H)-one moiety. The ^{13}C NMR data obtained for compound **4a** are in accordance with the 3,5-disubstituted isoxazoline regioisomer [28,55,56]. Moreover, the homonuclear ($^1\text{H}-^1\text{H}$) and heteronuclear ($^1\text{H}-^{13}\text{C}$) 2D NMR spectra of compound **4a** confirm unambiguously the assignment of the different signals made via the 1D NMR spectra (^1H and ^{13}C). The 2D NMR correlations are presented in Figures S8 and S9.

On the basis of the spectroscopic data, it can be concluded that the 1,3-dipolar cycloaddition reaction between allylated quinazolin-4(3H)-one **2** and aryl nitroxides led only to the formation of the 3,5-disubstituted isoxazoline regioisomer. To further explain the mechanism and the regiochemistry observed in this work, a theoretical study was carried out using the DFT/B3LYP method.

3.2. DFT Studies

The nucleophilic and electrophilic sites can be shown using the Mulliken atomic spin density analysis by observing the p^- and p^+ values [57,58].

Figure 4 shows a high value for p^- (0.455) in the reagent **3f** on the O1 atom compared to C3, which conveys a nucleophilic character for this site (O1), so a low value of p^+ on the same atom confirms this character. The sites C13 and C14 have almost the same values of p^- and p^+ , which means that they have almost the same nucleophile and electrophile characteristics. The C3 site has two low values of p^- and p^+ , while N2 has a remarkable electrophilic character (p^+ 0.172) and a very low value of p^- (0.06). This clearly explains a concerted mechanism for the 1,3-dipolar cycloaddition reaction.

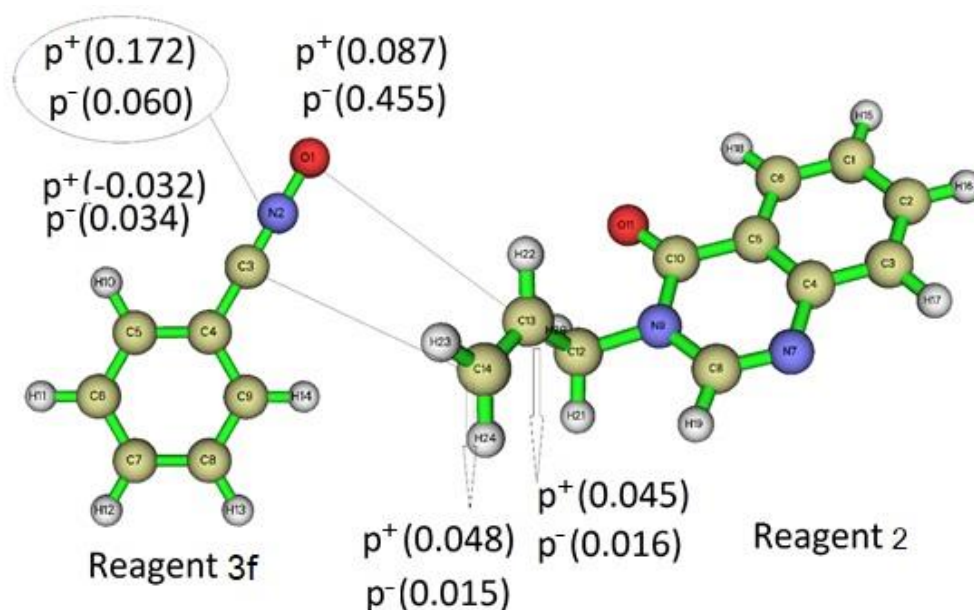


Figure 4. Nucleophilic p^- and Electrophilic p^+ functions of reagents **3f** and **2**.

The transition state structure (Figure 5) was localized following the Beryn algorithm. In this structure, the bond lengths of C16–C17 (2.231) and C13–O14 (2.379) show the beginning of a formation of two covalent bonds between C16–C17 and C13–O14. The negative value of the imaginary frequency confirms the localization of the transition state structure for this reaction.

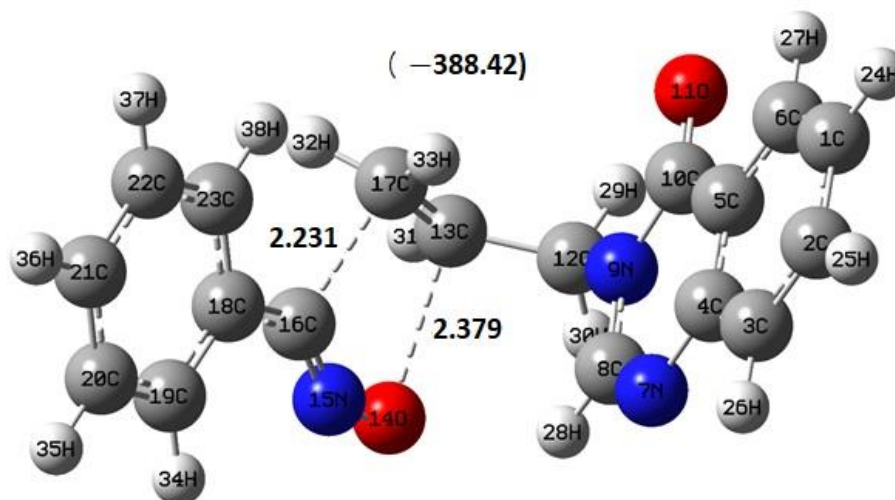


Figure 5. Transition state, length of the chemical bond, and, in parenthesis, imaginary frequency.

The kinetics and variables of the 1,3-dipolar cycloaddition reaction between dipole **3f** and dipolarophile **2** were investigated in order to disclose the more favorable product. It involves two electrons from the dipolarophile and four electrons from the 1,3-dipole. Figure 6 shows the energy profile corresponding to the cyclization mode. At the appropriate level of theory (B3LYP/cc-pVDZ), all reactants, transition states, and products were optimized.



Figure 6. Energy profiles for the 1,3-dipolar cycloaddition reaction between dipole **3f** and dipolarophile **2** at the B3LYP/cc-pVDZ in gas phase.

The IRC method (Figure 7) confirms the reaction pathway and shows that the product formed has a low energy compared to the starting materials. However, the transition state structure has a high energy relative to both the starting materials and the product.

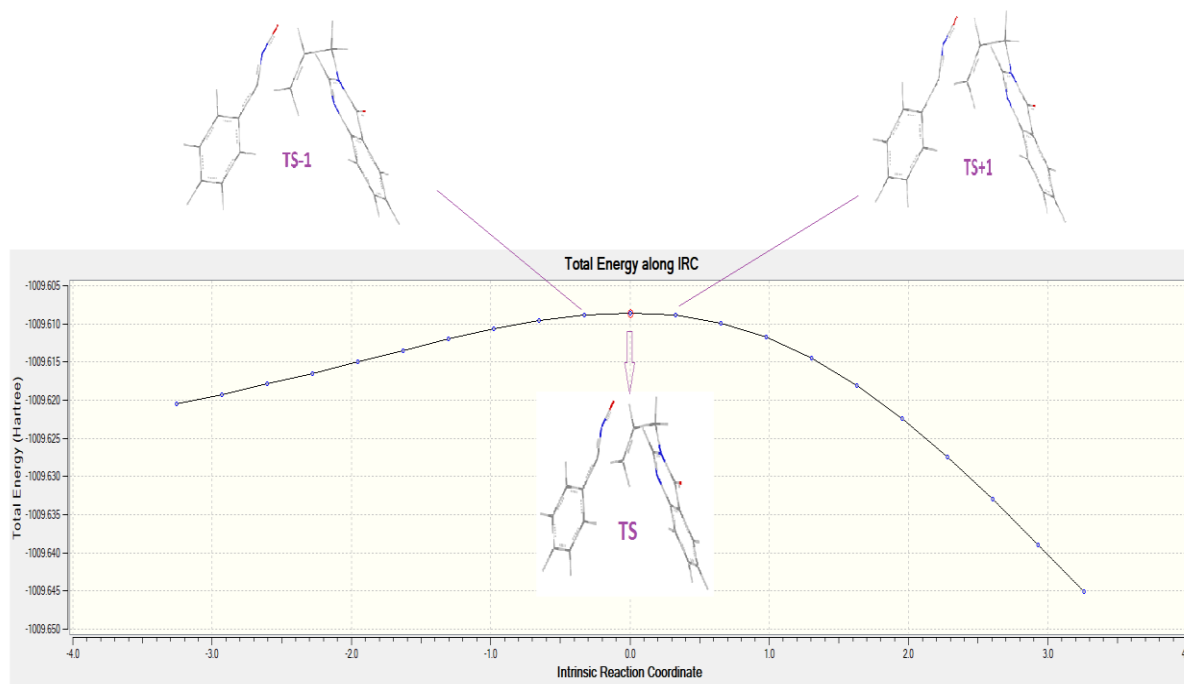


Figure 7. Intrinsic Reaction Coordinate and TS−1, TS and TS+1.

We have also shown the TS−1 structure, just before the transition structure, and the structure just after the TS (TS+1). This further justifies the location of the transition state.

The quantum theory of the atom in the molecule (QTAIM) is considered to be a technique giving a direct relationship between the distribution of the electron density $\rho(r)$ and the structure, which allows us to highlight the topology of the molecule. The presence of a critical point (3, −1) of an interatomic contour line indicates that the electron density is gathered among the nuclei. In Figure 8, BCP 67 and 82 show a chemical bond between C16–C17 and C13–O14 as the beginning of the formation of a new covalent bond.

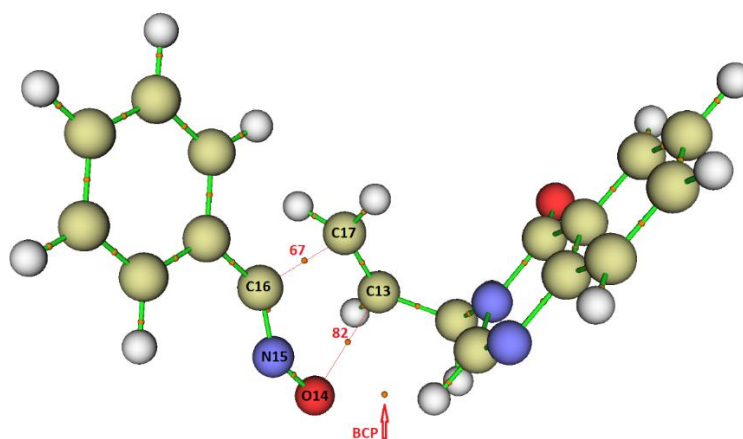


Figure 8. BCP Bond Critical Point (3, −1) for the two bonds C16–C17 and C13–O14 for compound TS.

The values shown in Table 2 for the electron density between C16–C17 (0.53) and a positive value of Laplacian (0.55) indicate a chemical gap in this interatomic region; the same applies for the C13–O14 bond.

Table 2. Electronic density and Laplacian for interactive bonding region.

	BCP	Bonding	ρ	$\nabla^2\rho$
TS	67	C16–C17	0.53	0.55
	82	C13–O14	0.33	0.83

The localized orbital localizer LOL was introduced by Schmider and Becke to describe the properties of the bond in terms of kinetic energy [59]. According to Figure 9, the green color between the two carbon atoms confirms the existence of a chemical bond in this region, and also shows a remarkable weak interaction between the carbon atom and the oxygen atom.

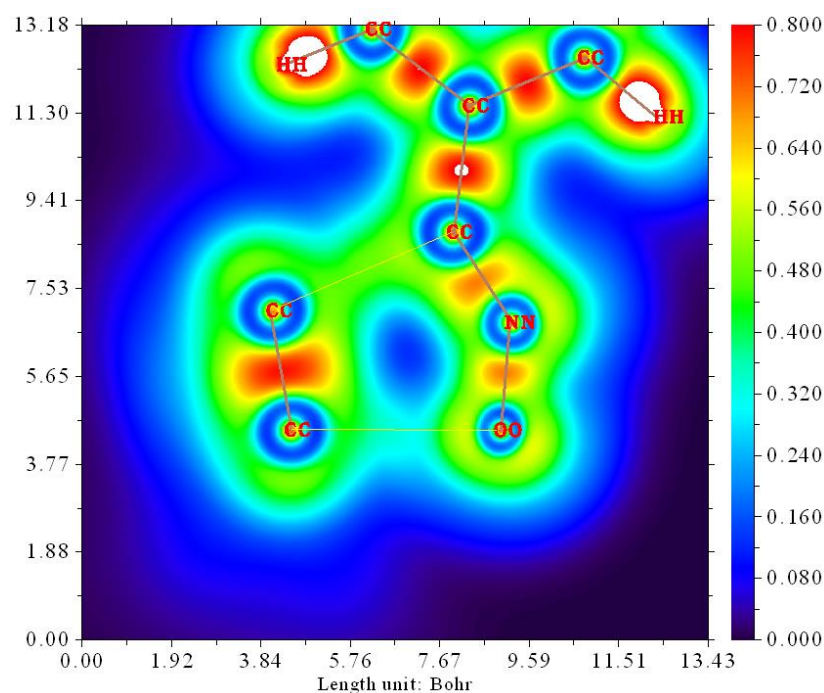


Figure 9. Map of functions LOL for the transition state.

From all of these findings, we can conclude that the outcomes of the computational study are in good agreement with the observed regiochemistry for the 1,3-dipolar cycloaddition between the aryl nitroxides and N-allylquinazolinone.

4. Conclusions

This study reports an efficient synthesis of a new series of hybrid molecules incorporating quinazolinone and isoxazoline cores through 1,3-dipolar cycloaddition reactions of N-allylquinazolinone with aryl nitroxides in a highly regioselective manner. The structures of the synthesized compounds were successfully established using spectroscopic techniques (IR, ^1H and ^{13}C NMR, and 2D NMR) and high-resolution mass spectrometry. The regiochemistry of the synthesized cycloadducts was proposed on the basis of the ^1H and ^{13}C NMR data and was further investigated using the DFT method. The computed results were in good agreement with the experimental data.

Supplementary Materials: The following supporting information can be downloaded at: <https://www.mdpi.com/article/10.3390/chemistry4030066/s1>. Spectroscopic data and copies of the spectra (^1H NMR, ^{13}C NMR, and HRMS) of all obtained compounds in this study can be found via the “Supplementary Content” section of this article’s webpage.

Author Contributions: Y.R. and M.C.: designed the experiments, analyzed the data, methodology, wrote—original draft, Wrote—review & editing. I.H. and S.C.: computational DFT and interpretation of results. M.A.: Spectroscopic analyses and interpretation of results. M.B.: English correction, validation of article and improve the manuscript, edited the final version. A.N. and M.E.Y.: conceptualization, methodology, manuscript preparation and review, validation of results, and supervision. All authors have read and agreed to the published version of the manuscript.

Funding: This research received no external funding.

Institutional Review Board Statement: Not applicable.

Informed Consent Statement: Not applicable.

Data Availability Statement: All data are mentioned in the manuscript.

Acknowledgments: The authors would like to thank the staff members of the “Cité de l’Innovation” of the Sidi Mohamed Ben Abdellah University for the IR, NMR and HRMS spectra recording.

Conflicts of Interest: The authors have no conflict of interest to declare that are relevant to the content of this article.

Sample Availability: Samples of the compounds **4a–h** are available from the authors.

References

1. Azimi, F.; Azizian, H.; Najafi, M.; Hassanzadeh, F.; Sadeghi-aliabadi, H.; Ghasemi, J.B.; Ali Faramarzi, M.; Mojtavavi, S.; Larijani, B.; Saghaei, L.; et al. Design and Synthesis of Novel Quinazolinone-Pyrazole Derivatives as Potential α -Glucosidase Inhibitors: Structure-Activity Relationship, Molecular Modeling and Kinetic Study. *Bioorganic Chem.* **2021**, *114*, 105127. [[CrossRef](#)] [[PubMed](#)]
2. Lee, J.Y.; Shin, Y.S.; Jeon, S.; Lee, S.I.; Noh, S.; Cho, J.E.; Jang, M.S.; Kim, S.; Song, J.H.; Kim, H.R.; et al. Design, Synthesis and Biological Evaluation of 2-Aminoquinazolin-4(3H)-One Derivatives as Potential SARS-CoV-2 and MERS-CoV Treatments. *Bioorganic Med. Chem. Lett.* **2021**, *39*, 127885. [[CrossRef](#)] [[PubMed](#)]
3. Rishikesan, R.; Karuvalam, R.P.; Muthipeedika, N.J.; Sajith, A.M.; Eeda, K.R.; Pakkath, R.; Haridas, K.R.; Bhaskar, V.; Narasimhamurthy, K.H.; Muralidharan, A. Synthesis of Some Novel Piperidine Fused 5-Thioxo-1H-1,2,4-Triazoles as Potential Antimicrobial and Antitubercular Agents. *J. Chem. Sci.* **2021**, *133*, 3. [[CrossRef](#)]
4. Kaushik, C.P.; Chahal, M. Synthesis and Antibacterial Activity of Benzothiazole and Benzoxazole-Appended Substituted 1,2,3-Triazoles. *J. Chem. Sci.* **2020**, *132*, 142. [[CrossRef](#)]
5. Jao, C.W.; Lin, W.C.; Wu, Y.T.; Wu, P.L. Isolation, Structure Elucidation, and Synthesis of Cytotoxic Tryptanthrin Analogues from *Phaius Mishmensis*. *J. Nat. Prod.* **2008**, *71*, 1275–1279. [[CrossRef](#)]
6. Sharma, S.; Kumar, D.; Singh, G.; Monga, V.; Kumar, B. Recent Advancements in the Development of Heterocyclic Anti-Inflammatory Agents. *Eur. J. Med. Chem.* **2020**, *200*, 112438. [[CrossRef](#)]
7. Ashok, D.; Reddy, M.R.; Dharavath, R.; Nagaraju, N.; Ramakrishna, K.; Gundu, S.; Sarasija, M. One-Pot Three-Component Condensation for the Synthesis of 2,4,6-Triarylpyridines and Evaluation of Their Antimicrobial Activity. *J. Chem. Sci.* **2021**, *133*, 22. [[CrossRef](#)]

8. Saeedi, M.; Mohammadi-Khanaposhtani, M.; Pourrabia, P.; Razzaghi, N.; Ghadimi, R.; Imanparast, S.; Faramarzi, M.A.; Bandarian, F.; Esfahani, E.N.; Safavi, M.; et al. Design and Synthesis of Novel Quinazolinone-1,2,3-Triazole Hybrids as New Anti-Diabetic Agents: In Vitro α -Glucosidase Inhibition, Kinetic, and Docking Study. *Bioorganic Chem.* **2019**, *83*, 161–169. [[CrossRef](#)] [[PubMed](#)]
9. El Abbouchi, A.; El Brahmī, N.; Hiebel, M.A.; Bignon, J.; Guillaumet, G.; Suzenet, F.; El Kazzouli, S. Synthesis and Evaluation of a Novel Class of Ethacrynic Acid Derivatives Containing Triazoles as Potent Anticancer Agents. *Bioorganic Chem.* **2021**, *115*, 105293. [[CrossRef](#)]
10. Faisal, M.; Saeed, A.; Hussain, S.; Dar, P.; Larik, F.A. Recent Developments in Synthetic Chemistry and Biological Activities of Pyrazole Derivatives. *J. Chem. Sci.* **2019**, *131*, 70. [[CrossRef](#)]
11. Kumar Pandey, S.; Yadava, U.; Upadhyay, A.; Sharma, M.L. Synthesis, Biological Evaluation and Molecular Docking Studies of Novel Quinazolinones as Antitubercular and Antimicrobial Agents. *Bioorganic Chem.* **2021**, *108*, 104611. [[CrossRef](#)] [[PubMed](#)]
12. Peng, J.W.; Yin, X.D.; Li, H.; Ma, K.Y.; Zhang, Z.J.; Zhou, R.; Wang, Y.L.; Hu, G.F.; Liu, Y.Q. Design, Synthesis, and Structure-Activity Relationship of Quinazolinone Derivatives as Potential Fungicides. *J. Agric. Food Chem.* **2021**, *69*, 4604–4614. [[CrossRef](#)] [[PubMed](#)]
13. Gatadi, S.; Lakshmi, T.V.; Nanduri, S. 4(3H)-Quinazolinone Derivatives: Promising Antibacterial Drug Leads. *Eur. J. Med. Chem.* **2019**, *170*, 157–172. [[CrossRef](#)]
14. Soliman, A.M.; Karam, H.M.; Mekki, M.H.; Ghorab, M.M. Antioxidant Activity of Novel Quinazolinones Bearing Sulfonamide: Potential Radiomodulatory Effects on Liver Tissues via NF-KB/PON1 Pathway. *Eur. J. Med. Chem.* **2020**, *197*, 112333. [[CrossRef](#)]
15. Ugale, V.G.; Bari, S.B.; Khadse, S.C.; Reddy, P.N.; Bonde, C.G.; Chaudhari, P.J. Exploring Quinazolinones as Anticonvulsants by Molecular Fragmentation Approach: Structural Optimization, Synthesis and Pharmacological Evaluation Studies. *ChemistrySelect* **2020**, *5*, 2902–2912. [[CrossRef](#)]
16. Zhu, S.; Wang, J.; Chandrashekar, G.; Smith, E.; Liu, X.; Zhang, Y. Synthesis and Evaluation of 4-Quinazolinone Compounds as Potential Antimalarial Agents. *Eur. J. Med. Chem.* **2010**, *45*, 3864–3869. [[CrossRef](#)]
17. Elshahawi, M.M.; EL-Ziaty, A.K.; Morsy, J.M.; Aly, A.F. Synthesis and Insecticidal Efficacy of Novel Bis Quinazolinone Derivatives. *J. Heterocycl. Chem.* **2016**, *53*, 1443–1448. [[CrossRef](#)]
18. Hu, Y.G.; Yang, S.J.; Ding, M.W. Synthesis and Fungicidal Activities of 2-Benzothiazolylthio-Substituted 4H-Imidazol-4-Ones and 4(3H)-Quinazolinones. *Phosphorus Sulfur Silicon Relat. Elem.* **2004**, *179*, 1933–1939. [[CrossRef](#)]
19. Alagarsamy, V.; Chitra, K.; Saravanan, G.; Solomon, V.R.; Sulthana, M.T.; Narendhar, B. An Overview of Quinazolines: Pharmacological Significance and Recent Developments. *Eur. J. Med. Chem.* **2018**, *151*, 628–685. [[CrossRef](#)]
20. Auti, P.S.; George, G.; Paul, A.T. Recent Advances in the Pharmacological Diversification of Quinazoline/Quinazolinone Hybrids. *RSC Adv.* **2020**, *10*, 41353–41392. [[CrossRef](#)]
21. Jahng, Y. Progress in the Studies on Tryptanthrin, an Alkaloid of History. *Arch. Pharm. Res.* **2013**, *36*, 517–535. [[CrossRef](#)] [[PubMed](#)]
22. Khan, I.; Ibrar, A.; Ahmed, W.; Saeed, A. Synthetic Approaches, Functionalization and Therapeutic Potential of Quinazoline and Quinazolinone Skeletons: The Advances Continue. *Eur. J. Med. Chem.* **2015**, *90*, 124–169. [[CrossRef](#)] [[PubMed](#)]
23. Kshirsagar, U.A. Recent Developments in the Chemistry of Quinazolinone Alkaloids. *Org. Biomol. Chem.* **2015**, *13*, 9336–9352. [[CrossRef](#)] [[PubMed](#)]
24. Gonçalves, I.L.; das Neves, G.M.; Porto Kagami, L.; Eifler-Lima, V.L.; Merlo, A.A. Discovery, Development, Chemical Diversity and Design of Isoxazoline-Based Insecticides. *Bioorganic Med. Chem.* **2021**, *30*, 115934. [[CrossRef](#)]
25. Asahi, M.; Kobayashi, M.; Kagami, T.; Nakahira, K.; Furukawa, Y.; Ozoe, Y. Fluxametamide: A Novel Isoxazoline Insecticide That Acts via Distinctive Antagonism of Insect Ligand-Gated Chloride Channels. *Pestic. Biochem. Physiol.* **2018**, *151*, 67–72. [[CrossRef](#)]
26. Romero-Núñez, C.; Bautista-Gómez, L.G.; Sheinberg, G.; Martín-Cordero, A.; Flores-Ortega, A.; Heredia-Cárdenas, R. Efficacy of Afoxolaner plus Milbemycin Oxime and Afoxolaner Alone as Treatment for Sarcoptic Mange in Naturally Infested Dogs. *Can. J. Vet. Res.* **2020**, *84*, 212–216.
27. Kreuzer, J.; Bach, N.C.; Forler, D.; Sieber, S.A. Target Discovery of Acivicin in Cancer Cells Elucidates Its Mechanism of Growth Inhibition. *Chem. Sci.* **2015**, *6*, 237–245. [[CrossRef](#)]
28. Filali, I.; Bouajila, J.; Znati, M.; Bousejra-El Garah, F.; Ben Jannet, H. Synthesis of New Isoxazoline Derivatives from Harmine and Evaluation of Their Anti-Alzheimer, Anti-Cancer and Anti-Inflammatory Activities. *J. Enzym. Inhib. Med. Chem.* **2015**, *30*, 371–376. [[CrossRef](#)]
29. Alshamari, A.; Al-Qudah, M.; Hamadeh, F.; Al-Momani, L.; Abu-Orabi, S. Synthesis, Antimicrobial and Antioxidant Activities of 2-Isoxazoline Derivatives. *Molecules* **2020**, *25*, 4271. [[CrossRef](#)]
30. Dadiboyena, S.; Nefzi, A. Solid Phase Synthesis of Isoxazole and Isoxazoline-Carboxamides via [2+3]-Dipolar Cycloaddition Using Resin-Bound Alkynes or Alkenes. *Tetrahedron Lett.* **2012**, *53*, 2096–2099. [[CrossRef](#)]
31. Kamal, A.; Bharathi, E.V.; Reddy, J.S.; Ramaiah, M.J.; Dastagiri, D.; Reddy, M.K.; Viswanath, A.; Reddy, T.L.; Shaik, T.B.; Pushpavalli, S.N.C.V.L.; et al. Synthesis and Biological Evaluation of 3,5-Diaryl Isoxazoline/Isoxazole Linked 2,3-Dihydroquinazolinone Hybrids as Anticancer Agents. *Eur. J. Med. Chem.* **2011**, *46*, 691–703. [[CrossRef](#)]
32. Chalkha, M.; Bakhouch, M.; Akhazzane, M.; Bourass, M.; Nicolas, Y.; Al Houari, G.; El Yazidi, M. Design, Synthesis and Characterization of Functionalized Pyrazole Derivatives Bearing Amide and Sulfonamide Moieties from Aza-Aurones. *J. Chem. Sci.* **2020**, *132*, 86. [[CrossRef](#)]

33. Bakhouch, M.; Al Houari, G.; Daoudi, M.; Kerbal, A.; Yazidi, M. El Michael Addition of Active Methylene Compounds to (Z)-2-Arylidenebenzo[b]Thiophen-3(2H)-Ones. *Mediterr. J. Chem.* **2015**, *4*, 9–17. [[CrossRef](#)]
34. Chalkha, M.; Akhazzane, M.; Moussaid, F.Z.; Daoui, O.; Nakkabi, A.; Bakhouch, M.; Chtita, S.; Elkhattabi, S.; Iraqi Housseini, A.; El Yazidi, M. Design, Synthesis, Characterization, in Vitro Screening, Molecular Docking, 3D-QSAR, and ADME-Tox Investigations of Novel Pyrazole Derivatives as Antimicrobial Agents. *New J. Chem.* **2022**, *46*, 2747–2760. [[CrossRef](#)]
35. Chalkha, M.; El Moussaoui, A.; Hadda, T.B.; Berredjem, M.; Bouzina, A.; Almalki, F.A.; Saghrouchni, H.; Bakhouch, M.; Saadi, M.; El Ammari, L.; et al. Crystallographic Study, Biological Evaluation and DFT/POM/Docking Analyses of Pyrazole Linked Amide Conjugates: Identification of Antimicrobial and Antitumor Pharmacophore Sites. *J. Mol. Struct.* **2022**, *1252*, 131818. [[CrossRef](#)]
36. Chalkha, M.; Nakkabi, A.; Hadda, T.B.; Berredjem, M.; El Moussaoui, A.; Bakhouch, M.; Saadi, M.; El Ammari, L.; Almalki, F.A.; Laaroussi, H.; et al. Crystallographic Study, Biological Assessment and POM/Docking Studies of Pyrazoles-Sulfonamide Hybrids (PSH): Identification of a Combined Antibacterial/Antiviral Pharmacophore Sites Leading to in-Silico Screening the Anti-COVID-19 Activity. *J. Mol. Struct.* **2022**, *1267*, 133605. [[CrossRef](#)]
37. Ouyang, G.; Zhang, P.; Xu, G.; Song, B.; Yang, S.; Jin, L.; Xue, W.; Hu, D.; Lu, P.; Chen, Z. Synthesis and Antifungal Bioactivities of 3-Alkylquinazolin-4-One Derivatives. *Molecules* **2006**, *11*, 383–392. [[CrossRef](#)]
38. Ribeiro, C.J.A.; Amaral, J.D.; Rodrigues, C.M.P.; Moreira, R.; Santos, M.M.M. Synthesis and Evaluation of Spiroisoxazoline Oxindoles as Anticancer Agents. *Bioorganic Med. Chem.* **2014**, *22*, 577–584. [[CrossRef](#)]
39. Becke, A.D. Density-functional Thermochemistry. I. The Effect of the Exchange-only Gradient Correction. *J. Chem. Phys.* **1992**, *96*, 2155–2160. [[CrossRef](#)]
40. Stecko, S.; Pańniczek, K.; Michel, C.; Milet, A.; Pérez, S.; Chmielewski, M. A DFT Study of 1,3-Dipolar Cycloaddition Reactions of 5-Membered Cyclic Nitrones with α,β -Unsaturated Lactones and with Cyclic Vinyl Ethers: Part 1. *Tetrahedron Asymmetry* **2008**, *19*, 1660–1669. [[CrossRef](#)]
41. Hammoudan, I.; Matchi, S.; Bakhouch, M.; Belaidi, S.; Chtita, S. QSAR Modelling of Peptidomimetic Derivatives towards HKU4-CoV 3CLpro Inhibitors against MERS-CoV. *Chemistry* **2021**, *3*, 391–401. [[CrossRef](#)]
42. Iron, M.A.; Martin, J.M.L.; Van der Boom, M.E. Cycloaddition Reactions of Metalloaromatic Complexes of Iridium and Rhodium: A Mechanistic DFT Investigation. *J. Am. Chem. Soc.* **2003**, *125*, 11702–11709. [[CrossRef](#)] [[PubMed](#)]
43. Heydari, S.; Haghdadi, M.; Hamzehloueian, M.; Bosra, H.G. An Investigation of the Regio-, Chemo-, and Stereoselectivity of Cycloaddition Reactions of 2-Phenylsulfonyl-1,3-Butadiene and Its 3-Phenylsulfonyl Derivative: A DFT Study. *Struct. Chem.* **2021**, *32*, 1819–1831. [[CrossRef](#)]
44. Zhang, I.Y.; Wu, J.; Xu, X. Extending the Reliability and Applicability of B3LYP. *Chem. Commun.* **2010**, *46*, 3057–3070. [[CrossRef](#)]
45. Haghdadi, M.; Nab, N.; Bosra, H.G. DFT Study on the Regio- and Stereo-Selectivity of the Diels-Alder Reaction between a Cycloprop-2-Ene Carboxylate and Some Cyclic 1,3-Dienes. *Prog. React. Kinet. Mech.* **2016**, *41*, 193–204. [[CrossRef](#)]
46. Hammoudan, I.; Chtita, S.; Riffi-Temsamani, D. QTAIM and IRC Studies for the Evaluation of Activation Energy on the C=P, C=N and C=O Diels-Alder Reaction. *Heliyon* **2020**, *6*, 3–7. [[CrossRef](#)] [[PubMed](#)]
47. Chamorro, E.; Pérez, P.; Domingo, L.R. On the Nature of Parr Functions to Predict the Most Reactive Sites along Organic Polar Reactions. *Chem. Phys. Lett.* **2013**, *582*, 141–143. [[CrossRef](#)]
48. Tighadouini, S.; Radi, S.; Roby, O.; Hammoudan, I.; Saddik, R.; Garcia, Y.; Almarhoon, Z.M.; Mabkhot, Y.N. Kinetics, Thermodynamics, Equilibrium, Surface Modelling, and Atomic Absorption Analysis of Selective Cu(II) Removal from Aqueous Solutions and Rivers Water Using Silica-2-(Pyridin-2-Ylmethoxy)Ethan-1-Ol Hybrid Material. *RSC Adv.* **2022**, *12*, 611–625. [[CrossRef](#)]
49. Laidler, K.J. The Development of the Arrhenius Equation. *J. Chem. Educ.* **1984**, *61*, 494–498. [[CrossRef](#)]
50. Boshala, A.; Said, M.A.; Assirey, E.A.; Alborki, Z.S.; AlObaid, A.A.; Zarrouk, A.; Warad, I. Crystal Structure, MEP/DFT/XRD, Thione \rightleftharpoons Thiol Tautomerization, Thermal, Docking, and Optical/TD-DFT Studies of (E)-Methyl 2-(1-Phenylethylidene)-Hydrazinecarbodithioate Ligand. *J. Mol. Struct.* **2021**, *1238*, 130461. [[CrossRef](#)]
51. Dupuis, M.; Chen, S.; Rauegi, S.; Dubois, D.L.; Bullock, R.M. Comment on “New Insights in the Electrocatalytic Proton Reduction and Hydrogen Oxidation by Bioinspired Catalysts: A DFT Investigation”. *J. Phys. Chem. A* **2011**, *115*, 4861–4865. [[CrossRef](#)] [[PubMed](#)]
52. Wick, C.R.; Clark, T. On Bond-Critical Points in QTAIM and Weak Interactions. *J. Mol. Model.* **2018**, *24*, 142. [[CrossRef](#)] [[PubMed](#)]
53. Frisch, M.J.; Trucks, G.W.; Schlegel, H.B.; Scuseria, G.E.; Robb, M.A.; Cheeseman, J.R.; Scalmani, G.; Barone, V.; Mennucci, B.; Petersson, G.A.; et al. *Gaussian 09, Revision C. 02*; Gaussian, Inc.: Wallingford, CT, USA, 2009.
54. Liu, K.-C.; Shelton, B.R.; Howe, R.K. A Particularly Convenient Preparation of Benzohydroximinoyl Chlorides (Nitrile Oxide Precursors). *J. Org. Chem.* **1980**, *45*, 3916–3918. [[CrossRef](#)]
55. Talha, A.; Favreau, C.; Bourgoin, M.; Robert, G.; Auberger, P.; El Ammari, L.; Saadi, M.; Benhida, R.; Martin, A.R.; Bougrin, K. Ultrasound-Assisted One-Pot Three-Component Synthesis of New Isoxazolines Bearing Sulfonamides and Their Evaluation against Hematological Malignancies. *Ultrason. Sonochem.* **2021**, *78*, 105748. [[CrossRef](#)]
56. Lobo, M.M.; Viau, C.M.; Dos Santos, J.M.; Bonacorso, H.G.; Martins, M.A.P.; Amaral, S.S.; Saffi, J.; Zanatta, N. Synthesis and Cytotoxic Activity Evaluation of Some Novel 1-(3-(Aryl-4,5-Dihydroisoxazol-5-Yl)Methyl)-4-Trihalomethyl-1H-Pyrimidin-2-Ones in Human Cancer Cells. *Eur. J. Med. Chem.* **2015**, *101*, 836–842. [[CrossRef](#)]
57. Domingo, L.R.; Pérez, P. Global and Local Reactivity Indices for Electrophilic/Nucleophilic Free Radicals. *Org. Biomol. Chem.* **2013**, *11*, 4350–4358. [[CrossRef](#)]

-
58. Domingo, L.R.; Pérez, P.; Sáez, J.A. Understanding the Local Reactivity in Polar Organic Reactions through Electrophilic and Nucleophilic Parr Functions. *RSC Adv.* **2013**, *3*, 1486–1494. [[CrossRef](#)]
 59. Schmider, H.L.; Becke, A.D. Chemical Content of the Kinetic Energy Density. *J. Mol. Struct. THEOCHEM* **2000**, *527*, 51–61. [[CrossRef](#)]